Bioorganic Chemistry 87 (2019) 447–456

Contents lists available at ScienceDirect

Bioorganic Chemistry

journal homepage: www.elsevier.com/locate/bioorg

Bioactive terpenoids from *Euonymus verrucosus* var. *pauciflorus* showing NO inhibitory activities

Yuling Yang[a,1], Xueyuan Yang[a,1], Xuke Zhang[a], Ziteng Song[a], Feng Liu[a], Yue Liang[a], Jie Zhang[b], Da-Qing Jin[c], Jing Xu[a,*], Dongho Lee[d], Muhetaer Tuerhong[e], Yasushi Ohizumi[f], Yuanqiang Guo[a,*]

[a] State Key Laboratory of Medicinal Chemical Biology, College of Pharmacy, and Tianjin Key Laboratory of Molecular Drug Research, Nankai University, Tianjin 300350, People's Republic of China
[b] Key Laboratory for Green Processing of Chemical Engineering of Xinjiang Bingtuan, School of Chemistry and Chemical Engineering, Shihezi University, Shihezi 832003, People's Republic of China
[c] School of Medicine, Nankai University, Tianjin 300071, People's Republic of China
[d] Department of Biosystems and Biotechnology, College of Life Sciences and Biotechnology, Korea University, Seoul 02841, Republic of Korea
[e] College of Chemistry and Environmental Sciences, Laboratory of Xinjiang Native Medicinal and Edible Plant Resources Chemistry, Kashgar University, Kashgar 844000, People's Republic of China
[f] Kansei Fukushi Research Institute, Tohoku Fukushi University, Sendai 989-3201, Japan

ARTICLE INFO

Keywords:
Euonymus verrucosus var. *pauciflorus*
Celastraceae
NO inhibitory activities
Norditerpenoids
iNOS

ABSTRACT

In our continuous search for new nitric oxide (NO) inhibitory compounds as potential anti-inflammatory agents or lead compounds for inflammatory diseases, the chemical constituents of *Euonymus verrucosus* var. *pauciflorus* were investigated, leading to the isolation of eleven terpenoids including six new diterpenoids, designated as euonymupenes A–F. The structures were elucidated on the basis of NMR and ECD data analysis. Euonymupenes A, C, and F feature rare labdane-type norditerpenoid skeletons. The NO inhibitory effects were evaluated and all of the isolates were found to inhibit lipopolysaccharide (LPS)-induced NO production in murine microglial BV-2 cells. Western blotting analysis indicated that the most active compound (**5**) can regulate iNOS (inducible nitric oxide synthase) expression. The further molecular docking studies exhibited the affinities of bioactive compounds with iNOS.

1. Introduction

Nitric oxide (NO), a signaling molecule, plays a significant role in many physiological and biochemical processes [1,2]. For the inflammatory response, an appropriate amount of NO contributes to an effective defense against pathogens, whereas overproduction of NO could stimulate the formation of some proinflammatory mediators and cause a series of subsequent inflammatory diseases [3,4]. Thus, to treat inflammatory disorders, NO inhibitors have been considered as an effective strategy. In addition to synthetic compounds with NO inhibitory effects, bioactive natural products with structural and biological diversity attracted the attention of medicinal researchers, which are a potential source of anti-inflammatory lead compounds [5,6].

The genus *Euonymus* L., belonging to the Celastraceae plant family, contains about 220 species distributed in the subtropical and temperate regions of the Western and Eastern Hemispheres [7]. There are about 110 species growing in China. Some *Euonymus* species have been well-known as folk medicines for various medical indications documented in medical books [8–11]. Terpenoids, especially sesquiterpenoids, flavonoids, alkaloids, steroids, and cardiac glycosides, have been reported from this genus and regarded as the major constituents, displaying a broad spectrum of biological effects, such as antitumor, hepatoprotective, anti-inflammatory, antioxidant, and neuroprotective activities [12–31]. The species *Euonymus verrucosus* var. *pauciflorus* is a deciduous shrub distributed mainly in Northeast China and the Korean Peninsula. There is no record on the medicinal purposes of this plant and no phytochemicals have been reported.

Considering that many bioactive substances have been discovered from the genus *Euonymus*, the species *E. verrucosus* var. *pauciflorus* unreported previously evoked our attention and its chemical constituents were investigated. The methanol extract of the twigs of *E. verrucosus* var. *pauciflorus* was fractionated, resulting in the isolation of eleven terpenoids including six new diterpenoids (**1**–**6**). The structures were established by analysis of NMR and electronic circular dichroism (ECD)

* Corresponding authors.
E-mail addresses: xujing611@nankai.edu.cn (J. Xu), victgyq@nankai.edu.cn (Y. Guo).
[1] These authors contributed equally to this work.

https://doi.org/10.1016/j.bioorg.2019.03.022
Received 31 December 2018; Received in revised form 16 February 2019; Accepted 11 March 2019
Available online 15 March 2019
0045-2068/

Table 1
^{13}C NMR data for compounds **1–6** (δ in ppm, 100 MHz, in $CDCl_3$).[a]

Position	1	2	3	4	5	6
1	42.2, CH_2	42.2, CH_2	43.8, CH_2	43.9, CH_2	42.1, CH_2	41.9, CH_2
2	19.5, CH_2	19.4, CH_2	19.2, CH_2	19.3, CH_2	19.5, CH_2	19.4, CH_2
3	43.8, CH_2	43.8, CH_2	43.9, CH_2	44.0, CH_2	43.9, CH_2	43.8, CH_2
4	34.5, C	34.4, C	34.5, C	34.5, C	34.4, C	34.4, C
5	57.3, CH	57.1, CH	56.6, CH	56.8, CH	57.3, CH	57.0, CH
6	69.2, CH	69.2, CH	68.7, CH	69.0, CH	69.2, CH	69.1, CH
7	47.4, CH_2	47.1, CH_2	46.4, CH_2	46.5, CH_2	47.5, CH_2	47.0, CH_2
8	144.0, C	145.1, C	144.4, C	145.9, C	144.0, C	144.6, C
9	57.1, CH	51.6, CH	61.5, CH	62.5, CH	57.9, CH	52.9, CH
10	40.7, C	40.1, C	40.5, C	40.2, C	40.9, C	39.9, C
11	24.3, CH_2	36.2, CH_2	148.4, CH	130.8, CH	22.8, CH_2	30.7, CH_2
12	155.6, CH	194.3, C	126.1, CH	127.0, CH	138.7, CH	179.5, C
13	139.2, C	128.1, C	195.0, C	137.9, C	136.8, C	
14	195.2, CH	108.8, CH	52.9, CH	126.3, CH	136.7, CH	
15		144.2, CH	46.2, CH_2	58.6, CH_2	111.5, CH_2	
16	9.4, CH_3	146.8, CH		64.7, CH_2	57.0, CH_2	
17	111.5, CH_2	110.1, CH_2	112.4, CH_2	111.8, CH_2	111.6, CH_2	110.4, CH_2
18	33.7, CH_3	33.6, CH_3	33.6, CH_3	33.6, CH_3	33.7, CH_3	33.6, CH_3
19	23.7, CH_3	23.7, CH_3	23.8, CH_3	23.8, CH_3	23.6, CH_3	23.6, CH_3
20	17.2, CH_3	17.6, CH_3	18.1, CH_3	18.2, CH_3	17.2, CH_3	17.2, CH_3

[a] Assignments of ^{13}C NMR data are based on DEPT, HMQC, and HMBC experiments.

data. Compounds **1**, **3**, and **6** feature rare labdane-type norditerpenoid skeletons. Herein, we describe the structural determination and NO inhibitory effects of these isolated labdane diterpenoids as well as their mechanism of anti-inflammatory effects.

2. Experimental section

2.1. General experimental procedures

Optical rotations were recorded on an InsMark IP120 automatic polarimeter (InsMark Instrument Co., Ltd., Shanghai, People's Republic of China). ECD spectra were obtained on a JASCO J-715 CD spectrometer (JASCO Corporation, Tokyo, Japan). Infrared (IR) spectra were recorded on a Bruker Tensor 27 FT-IR spectrometer. 1D and 2D NMR experiments were performed on a Bruker AV 400 instrument (Bruker, Switzerland, 100 MHz for ^{13}C and 400 MHz for ^{1}H) with TMS as an internal reference at room temperature. High resolution (HR)-ESIMS were recorded by ACQUITY UPLC I-Class SYNAPT G2-Si HDMS (Waters Corp. UK). HPLC separations were conducted on a CXTH system, equipped with a Shodex RI-102 detector (Showa Denko Co., Ltd., Tokyo, Japan) and a YMC-pack ODS-AM (20 × 250 mm) column (YMC Co. Ltd., Kyoto, Japan). Medium pressure liquid chromatography (MPLC) was run on a P0100 pump with an ultraviolet (UV) detector (Huideyi Co., Beijing, People's Republic of China) and a column (40 × 400 mm) filled by octadecylsilyl (ODS, 50 μm, YMC Co., Ltd.). Silica gel (200–300 mesh) used for column chromatography was purchased from Qingdao Haiyang Chemical Group Co., Ltd. (Qingdao, People's Republic of China). Chemical reagents (analytical grade) and biological reagents were provided by Tianjin Chemical Reagent Co. (Tianjin, People's Republic of China) and Sigma Co., respectively. The BV-2 cell line was from Shanghai Institutes for Biological Sciences, Chinese Academy of Sciences (Shanghai, People's Republic of China).

2.2. Plant material

The twigs of *E. verrucosus* var. *pauciflorus* were collected from Changbai Mountain, Jilin Province, People's Republic of China, in August 2015. The botanical identification was made by one of the authors (Y. Guo), State Key Laboratory of Medicinal Chemical Biology, College of Pharmacy, and Tianjin Key Laboratory of Molecular Drug Research, Nankai University. A voucher specimen (No. 20150803) was deposited at the laboratory, College of Pharmacy, Nankai University.

2.3. Extraction and isolation

The twigs of *E. verrucosus* var. *pauciflorus* (10.5 kg) were cut into pieces. After air-drying, these pieces were extracted with methanol (3 × 60 L) under reflux. The organic solvent was evaporated to afford a residue (450 g). This residue was dissolved in H_2O (0.5 L) and partitioned with ethyl acetate (3 × 0.5 L). The resulting ethyl acetate soluble-portion (146 g) was subjected to silica gel chromatography (silica gel, 0.7 kg; column, 7 × 50 cm) using a gradient solvent system of petroleum ether-acetone (100: 0, 100: 2, 100: 4, 100: 6, 100: 9, 100: 13, 100: 30, and 100: 40, 14 L for each gradient elution), to yield seven fractions (F_1–F_7) after TLC analysis. Fraction F_2 (8.5 g) was fractionated by MPLC over ODS (64–94% MeOH in H_2O) to give five subfractions $F_{2\text{-}1}$–$F_{2\text{-}5}$. Subfraction $F_{2\text{-}3}$ was further purified by preparative HPLC (YMC-pack ODS-AM column, 20 × 250 mm, 83% MeOH in H_2O) to provide compounds **1** (t_R = 27 min, 5.4 mg) and **3** (t_R = 35 min, 17.7 mg). Using the same HPLC, subfraction $F_{2\text{-}4}$ (87% MeOH in H_2O) provided compounds **2** (t_R = 30 min, 7.6 mg), **7** (t_R = 29 min, 9.8 mg), and **11** (t_R = 41 min, 10 mg). Subfraction $F_{2\text{-}5}$ was further purified by the above HPLC (94% MeOH in H_2O) to yield compound **8** (t_R = 24 min, 18.6 mg). Fraction F_6 (19.0 g) was fractionated by the same MPLC to afford six subfractions $F_{6\text{-}1}$–$F_{6\text{-}6}$, and the purification of $F_{6\text{-}2}$ by the same HPLC (69% MeOH in H_2O) led to the isolation of compound **4** (t_R = 44 min, 6.2 mg). With the above MPLC, fraction F_3 (11.5 g, 62–91% MeOH in H_2O) gave nine subfractions $F_{3\text{-}1}$–$F_{3\text{-}9}$. Compound **5** (t_R = 38 min, 15.7 mg) was acquired from subfraction $F_{3\text{-}6}$ (82% MeOH in H_2O) by the above HPLC, and the purification of $F_{3\text{-}2}$ (66% MeOH in H_2O) resulted in the isolation of compounds **9** (t_R = 35 min, 11 mg) and **10** (t_R = 39 min, 7.7 mg). Through the same procedures as for F_3, fraction F_4 (13.0 g) yielded seven subfractions $F_{4\text{-}1}$–$F_{4\text{-}7}$. Compound **6** (t_R = 52 min, 26.6 mg) was isolated from $F_{4\text{-}2}$ (69% MeOH in H_2O) by the same HPLC.

Euonymupene A (1): colorless oil; $[\alpha]_D^{26}$ −1.6 (*c* 0.4, CH_2Cl_2); ECD (CH_3CN) 202 ($\Delta\varepsilon$ −3.43), 235 ($\Delta\varepsilon$ +1.37) nm; IR (film) ν_{max}: 3486, 2924, 2847, 1713, 1680, 1563, 1460, 1385, 1293, 1188, 1080, 972, 893, 780 cm^{-1}; ^{1}H NMR (400 MHz, $CDCl_3$) and ^{13}C NMR (100 MHz, $CDCl_3$) data, see Tables 1 and 2; ESIMS *m/z* 291 $[M+H]^+$; HRESIMS *m/z* 291.2321 $[M+H]^+$, calcd for $C_{19}H_{31}O_2$, 291.2324.

Euonymupene B (2): colorless crystal; mp 131–133 °C; $[\alpha]_D^{26}$ −28.2 (*c* 0.3, CH_2Cl_2); ECD (CH_3CN) 192 ($\Delta\varepsilon$ −4.08), 202 ($\Delta\varepsilon$ −2.57), 208 ($\Delta\varepsilon$ −2.89), 231 ($\Delta\varepsilon$ −1.08), 246 ($\Delta\varepsilon$ −1.15), 321 ($\Delta\varepsilon$ −0.07) nm; IR (film) ν_{max}: 3527, 3125, 3095, 2955, 2920, 2843, 1770, 1616, 1557, 1461, 1327, 1219, 1114, 1033, 975, 889, 775, 642 cm^{-1}; ^{1}H NMR

Table 2
^{1}H NMR data for compounds **1–6** (δ in ppm, J in Hz, 400 MHz, in $CDCl_3$).[a]

Position	1	2	3	4	5	6
1α	1.12 m	1.19 m	1.12 m	1.15 m	1.13 m	1.18 m
1β	1.79 m	1.57 m	1.59 m	1.58 m	1.79 m	1.58 m
2α	1.50 m	1.49 m	1.43 m	1.41 m	1.51 m	1.50 m
2β	1.73 m	1.65 m	1.61 m	1.64 m	1.66 m	1.61 m
3α	1.77 m	1.21 m	1.15 m	1.19 m	1.19 m	1.18 m
3β	1.44 m	1.39 m	1.41 m	1.41 m	1.38 m	1.38 m
5	1.14 m[b]	1.23 m[b]	1.09 m[b]	1.11 m[b]	1.10 m[b]	1.17 m[b]
6	4.41 br s	4.42 br s	4.41 br s	4.40 br s	4.39 s	4.41 br s
7α	2.38 m[b]	2.36 d (13.5)	2.39 m[b]	2.41 m	2.34 m[b]	2.34 m[b]
7β		2.49 d (13.3)				2.43 m[b]
9	1.96 d (11.0)	2.69 d (9.5)	2.53 d (10.4)	2.44 d (10.1)	1.82 m	2.38 m
11a	2.43 m	2.79 dd (16.8, 2.6)	7.28 dd (15.6, 10.4)	5.98 dd (15.3, 10.1)	2.49 dd (17.6, 6.9)	2.53 m
11b	2.62 m	3.02 dd (16.8, 10.0)			2.30 dd (10.9, 4.8)	2.41 m
12	6.45 t (6.6)		6.25 d (15.6)	5.76 br s	6.26 dd (17.7, 10.9)	
14	9.36 s	6.78 s	3.58 dd (4.4, 2.4)	6.24 d (15.7)	5.61 t (6.8)	
15a		7.44 s	3.06 t (5.3)	4.34 m	5.29 d (17.6)	
15b			2.89 dd (5.8, 2.4)		5.02 d (10.8)	
16	1.78 s	8.09 s		4.34 s	4.36 m	
17a	4.68 s	4.65 s	4.69 s	4.74 s	4.77 s	4.81 s
17b	5.02 s	4.89 s	4.96 s	4.93 s	5.02 s	4.95 s
18	1.02 s	1.02 s	1.02 s	1.02 s	1.01 s	1.01 s
19	1.23 s	1.22 s	1.23 s	1.23 s	1.21 s	1.20 s
20	1.08 s	1.09 s	1.21 s	1.14 s	1.04 s	1.01 s

[a] Assignments of ^{1}H NMR data are based on ^{1}H-^{1}H COSY, HMQC, and HMBC experiments.
[b] Signals are in overlapped regions of the spectra and the multiplicities could not be discerned.

(400 MHz, $CDCl_3$) and ^{13}C NMR (100 MHz, $CDCl_3$) data, see Tables 1 and 2; ESIMS m/z 317 $[M+H]^+$; HRESIMS m/z 317.2117 $[M+H]^+$, calcd for $C_{20}H_{29}O_3$, 317.2117.

Euonymupene C (***3***): colorless oil; $[\alpha]_D^{26}$ −8.0 (c 0.2, CH_2Cl_2); ECD (CH_3CN) 202 ($\Delta\varepsilon$ −3.43), 240 ($\Delta\varepsilon$ +1.19) nm; IR (film) ν_{max}: 3420, 3082, 2924, 2865, 2844, 1708, 1645, 1459, 1386, 1265, 1112, 1031, 993, 869, 735 cm^{-1}; ^{1}H NMR (400 MHz, $CDCl_3$) and ^{13}C NMR (100 MHz, $CDCl_3$) data, see Tables 1 and 2; ESIMS m/z 305 $[M+H]^+$; HRESIMS m/z 305.2115 $[M+H]^+$, calcd for $C_{19}H_{29}O_3$, 305.2117.

Euonymupene D (***4***): colorless oil; $[\alpha]_D^{26}$ −9.0 (c 0.2, CH_2Cl_2); ECD (CH_3CN) 200 ($\Delta\varepsilon$ −4.23), 229 ($\Delta\varepsilon$ +1.38) nm; IR (film) ν_{max}: 3380, 2923, 2865, 2851, 1581, 1461, 1380, 1265, 1034, 993, 865, 778 cm^{-1}; ^{1}H NMR (400 MHz, $CDCl_3$) and ^{13}C NMR (100 MHz, $CDCl_3$) data, see Tables 1 and 2; ESIMS m/z 321 $[M+H]^+$; HRESIMS m/z 321.2433 $[M+H]^+$, calcd for $C_{20}H_{33}O_3$, 321.2430.

Euonymupene E (***5***): colorless oil; $[\alpha]_D^{26}$ +6.8 (c 0.2, CH_2Cl_2); ECD (CH_3CN) 202 ($\Delta\varepsilon$ −2.82), 231 ($\Delta\varepsilon$ +1.33) nm; IR (film) ν_{max}: 3420, 3082, 2924, 2944, 1645, 1459, 1386, 1265, 1076, 993, 869, 735 cm^{-1}; ^{1}H NMR (400 MHz, $CDCl_3$) and ^{13}C NMR (100 MHz, $CDCl_3$) data, see Tables 1 and 2; ESIMS m/z 305 $[M+H]^+$; HRESIMS m/z 305.2478 $[M+H]^+$, calcd for $C_{20}H_{33}O_2$, 305.2481.

Euonymupene F (***6***): colorless oil; $[\alpha]_D^{26}$ −32.9 (c 0.3, CH_2Cl_2); ECD (CH_3CN) 206 ($\Delta\varepsilon$ −0.25) nm; IR (film) ν_{max}: 3482, 3080, 2994, 2867, 1648, 1458, 1363, 1248, 1055, 976, 865, 737 cm^{-1}; ^{1}H NMR (400 MHz, $CDCl_3$) and ^{13}C NMR (100 MHz, $CDCl_3$) data, see Tables 1 and 2; ESIMS m/z 267 $[M+H]^+$; HRESIMS m/z 267.1963 $[M+H]^+$, calcd for $C_{16}H_{27}O_3$, 267.1960.

2.4. Computational method

According to the configuration of every compound deduced from the NOESY spectra and Chem3D modeling, systematic conformation searches were performed firstly using MOE software and appropriate conformers were selected for geometry optimizations. Geometry optimizations and re-optimizations on the B3LYP/6-31 + G(d) level were performed by the Gaussian 09 package [32,33]. The TDDFT ECD calculations for the optimized conformers were carried out at the CAM-B3LYP/SVP level with a CPCM solvent model in acetonitrile, and the calculated ECD spectra of different conformers were simulated with a half bandwidth of ~0.4 eV. The ECD curves were extracted by SpecDis 1.62 software [34]. The overall ECD curves of all the compounds were weighted by Boltzmann distribution after UV correction.

2.5. Bioassay for NO production in LPS-induced murine microglial BV-2 cells

NO is an important inflammatory factor and the NO inhibitory effects of these compounds were examined by inhibiting NO release in LPS-induced murine microglial BV-2 cells. The cells were cultured at 37 °C in DMEM supplemented with 10% (v/v) inactivated fetal bovine serum and 100 U/mL penicillin/streptomycin under a water-saturated atmosphere of 95% air and 5% CO_2. The cells were seeded in 96-well culture plates (5×10^4 cells/well) and allowed to adhere for 24 h at 37 °C. The cells were incubated for 20 h with or without 0.2 μg/mL of LPS (Sigma Chemical Co., St. Louis, MO, U.S.A.) in the absence or presence of the test compounds. 2-Methyl-2-thiopseudourea, sulfate (SMT) was used as a positive control. As a parameter of NO synthesis, the nitrite concentration was measured by the Griess reaction using the supernatant of the BV-2 cells. Briefly, 50 μL of the cell culture supernatant were reacted with 50 μL of Griess reagent [1: 1 mixture of 0.1% *N*-(1-naphtyl) ethylenediamine in H_2O and 1% sulfanilamide in 5% phosphoric acid] in a 96 well plate and the absorbance was read with a microplate reader (Thermo Fisher Scientific Inc. America) at 550 nm. The experiment was performed three times, and the IC_{50} values for the inhibition of NO production were determined using the software SPSS11.5 from the corresponding experimental data.

2.6. Western blotting analysis

Western blotting analysis experiments were performed according to the method reported in the literature [35,36]. BV-2 cells were seeded in 12-well plates at a density of 3×10^5 cells/well. After incubation for 24 h, the cells were pretreated with compound **5** for 30 min, and then were stimulated with LPS (0.2 μg/mL). After a continuous incubation for 16 h, cells were washed with cold PBS twice and collected. The cells were suspended in lysis buffer for 1 h. The lysates were then centrifuged at 10,000 rpm for 10 min and the supernatants were collected. The protein concentration in lysis buffer was quantified by BCA protein

assay kit. (Solarbio, Beijing, People's Republic of China). Equal amounts of proteins (20 μg) were separated by SDS-PAGE gel electrophoresis and transferred to polyvinylidene difluoride membranes. The membrane was blocked with 5% skim milk for 2 h and then incubated with primary antibody overnight. After thoroughly washing with TBST, horseradish peroxidase-conjugated secondary antibodies (1: 5000 dilution in 5% skim milk) were applied and the blots were developed using an ECL detection kit. (Beyotime, Shanghai, People's Republic of China).

2.7. Molecular docking experiments

Molecular docking simulations were performed using the software AutoDock Vina along with AutoDock Tools (ADT 1.5.6) using the hybrid Lamarckian Genetic Algorithm (LGA). The three dimensional (3D) crystal structure of iNOS (PDB code, 3E6T) was obtained from the RCSB Protein Data Bank, whose resolution was 2.5 Å [37]. The standard 3D structures (PDB format) of selected compounds for molecular docking were constructed by chem3D Pro 14.0 software, whose configurations were determined by their NOESY spectra and Chem3D modeling. The cubic grid box of 20 Å size (x, y, z) with a spacing of 1.000 Å and grid maps were built [38,39]. All of the other parameters were used according to default settings of AutoDock Vina. Results differing by less than 2.0 Å in positional root mean-square deviation (RMSD) were clustered together, and the results of the most favorable free energy of binding were chosen as the resultant complex structures.

3. Results and discussion

3.1. Structure determination of new and known compounds

The ethyl acetate-soluble portion of the methanol extract of the twigs of *E. verrucosus* var. *pauciflorus* was fractionated by column chromatography and purified by HPLC to obtain six new labdane-type diterpenoids or norditerpenoids (**1–6**) and five known compounds (Fig. 1).

Compound **1** was obtained as a colorless oil. Its molecular formula was determined to be $C_{19}H_{30}O_2$ from the HRESIMS ion peak at *m/z* 291.2321 $[M+H]^+$ (calcd for $C_{19}H_{31}O_2$, 291.2324), which was consistent with its ^1H and ^{13}C NMR data (Tables 1 and 2). The ^1H NMR spectra of **1** exhibited signals for three aliphatic methyl singlets (δ_H 1.02, 1.23, and 1.08), one olefinic methyl singlet (δ_H 1.78), three olefinic protons [δ_H 6.45 (1H, t, J = 6.6 Hz), and 4.68 and 5.02 (each 1H, s)], and one aldehyde proton [δ_H 9.36 (1H, s)]. The ^{13}C NMR spectrum showed 19 carbon resonances (Table 1) comprising four methyls [δ_C 9.4 (C-16), 17.2 (C-20), 23.7 (C-19), and 33.7 (C-18)], six methylenes [δ_C 19.5 (C-2), 24.3 (C-11), 42.2 (C-1), 43.8 (C-3), 47.4 (C-7), and 111.5 (C-17)], five methines [δ_C 57.1 (C-9), 57.3 (C-5), 69.2 (C-6), 155.6 (C-12), and 195.2 (C-14)], and four quaternary carbons [δ_C 34.5 (C-4), 40.7 (C-10), 139.2 (C-13), and 144.0 (C-8)] with the aid of DEPT and HMQC spectra. The following HMBC and ^1H-^1H COSY experiments were preformed to determine the structure of **1**. The HMBC spectrum showed the long-range correlations of H_3-20 to C-1, C-5, C-9, and C-10, H_3-18/19 to C-3, C-4, and C-5, H-6 to C-4, C-5, C-7, C-8, and C-10, H_2-17 to C-7, C-8, and C-9, together with the ^1H-^1H COSY correlations of H_2-1/H_2-2/H_2-3 (Fig. 2), indicated the presence of two six-membered rings A and B, which carried one exocyclic terminal double bond $\Delta^{8,17}$, a hydroxy group attached at C-6, and three methyl groups (Me-18, Me-19, and Me-20) at C-4, C-4, and C-10, respectively. Apart from the two six-membered rings A and B, a side chain consisting of five carbons (δ_C 195.2, 155.6, 139.2, 24.3, and 9.4) was deduced and determined as shown in Fig. 2 by interpretation of the HMBC and ^1H-^1H COSY data, where the olefinic and aldehyde signals at δ_C 155.6, 139.2, and 195.2 were attributed to C-12, C-13, and C-14, respectively. This side chain was corroborated to be linked to C-9 of the ring B by the ^1H-^1H COSY couplings of H-9/H_2-11/H-12 and HMBC correlations of H-9 to C-11 and C-12, and H_2-11 to C-8–C-10. All of the above spectroscopic data analysis led to the planar structure of **1** to be elucidated as depicted in Fig. 1, which was a labdane-type 15-norditerpenoid.

The relative configuration of compound **1** was deduced from the NOESY spectrum and Chem3D modeling (Fig. 3). NOESY interactions observed for H_3-20/H-1β, H_3-20/H-2β, H-9/H-7α, H-7α/H-6, H_3-18/H-5, H-5/H-9, and H-12/H-14, together with Chem3D modeling, implied a conformation for compound **1** as depicted in Fig. 3, where two six-membered rings A and B both presented chair conformations and were *trans*-fused with H-5 in an α-axail position and Me-20 in a β-axial position [40]. In turn, an α-axial orientation for H-9, a β-axial orientation for Me-19, and an *E*-configuration for Δ^{12} were determined according to the corresponding NOESY correlations. The C-6 hydroxy group was assigned as being in β-axial position, which was also supported by the coupling constant between H-6 and H-5 ($J_{5,6}$ = ~0 Hz). The absolute configuration of **1** was established by the TDDFT method, a tool applied extensively to assign the absolute configurations of natural products [41,42]. Based on the relative configuration of **1** deduced from its NOESY spectrum and Chem3D modelling, conformation searches with the MMFF94 force field by MOE software and the following geometry optimizations by the Gaussian 09 package were carried out. Then, the ECD calculations at the CAM-B3LYP/SVP level with the CPCM model were performed. The calculated ECD spectrum of **1** (Fig. 4) matched the experimental results closely, which suggested an absolute configuration of 5*S*, 6*R*, 9*S*, and 10*R* for compound **1**. On the basis of the above analysis, the structure of compound **1** was characterized unambiguously as shown in Fig. 1, and this compound was named euonymupene A.

Compound **2** was obtained as a colorless crystal. Its molecular formula was determined to be $C_{20}H_{28}O_3$ through the presence of a HRESIMS ion at *m/z* 317.2117 $[M+H]^+$ (calcd for $C_{20}H_{29}O_3$, 317.2117). From the ^1H and ^{13}C NMR spectra of **2**, the olefinic proton signals [δ_H 6.78 (1H, s, H-14), 7.44 (1H, s, H-15), 8.09 (1H, s, H-16)], and the characteristic carbon signals [δ_C 128.1 (C-13), 108.8 (C-14), 144.2 (C-15), and 146.8 (C-16)] revealed the presence of a β-substituted furan ring. Apart from these signals for the furan ring moiety, the ^1H NMR spectrum showed signals attributable to three aliphatic singlets [δ_H 1.02 (H_3-18), 1.22 (H_3-19), and 1.09 (H_3-20)], two olefinic protons [δ_H 4.65 and 4.89 (each 1H, s, H_2-17)], and one oxymethine proton [δ_H 4.42 (s, H-6)]. The ^{13}C NMR spectrum displayed additional 16 carbon signals, which were sorted as three methyls, six methylenes [one olefinic methylene (δ_C 110.1)], three methines [one oxymethine (δ_C 69.2)], and four quaternary carbons [one ketone carbonyl (δ_C 194.3) and one olefinic carbon (δ_C 145.1)], based on the DEPT and HMQC experiments. The subsequent HMBC and ^1H-^1H COSY experiments were performed to elucidate the structure. Analysis of 1D and 2D NMR spectra disclosed the 6/6 fused bicyclic fragment consisting of C-1–C-10 and C-17–C-20 (Fig. 2), which was the same as that of compound **1**. After finishing the assignments of the proton and carbon signals in the above-mentioned furan ring and 6/6 fused bicyclic fragment, it was found that there were two carbon signals left including one ketone carbonyl (δ_C 194.3) and one methylene (δ_C 36.2). The two carbon signals were assigned to C-11 and C-12, which connected the furan ring and the 6/6 fused bicyclic fragment. The planar structure of **2** was thus established as shown in Fig. 1, which possessed the same 6/6 fused bicyclic fragment as compound **1**. The following NOESY experiment revealed that the 6/6 fused bicyclic fragment in **2** had the same conformation as that of compound **1**. After defining the relative configuration, the absolute configuration of compound **2** was established to be 5*S*, 6*R*, 9*S*, and 10*R*, by comparison of the experimental and calculated ECD data (Fig. 4). On the basis of the above evidence, the structure of **2** was elucidated as shown, and the compound, a new diterpenoid, was named euonymupene B.

Compound **3**, a colorless oil, possesssed a molecular formula as $C_{19}H_{28}O_3$ based on its NMR data (Tables 1 and 2) and the HRESIMS ion at *m/z* 305.2115 $[M+H]^+$ (calcd for $C_{19}H_{29}O_3$, 305.2117). The ^1H NMR spectra exhibited signals for three aliphatic methyl singlets and

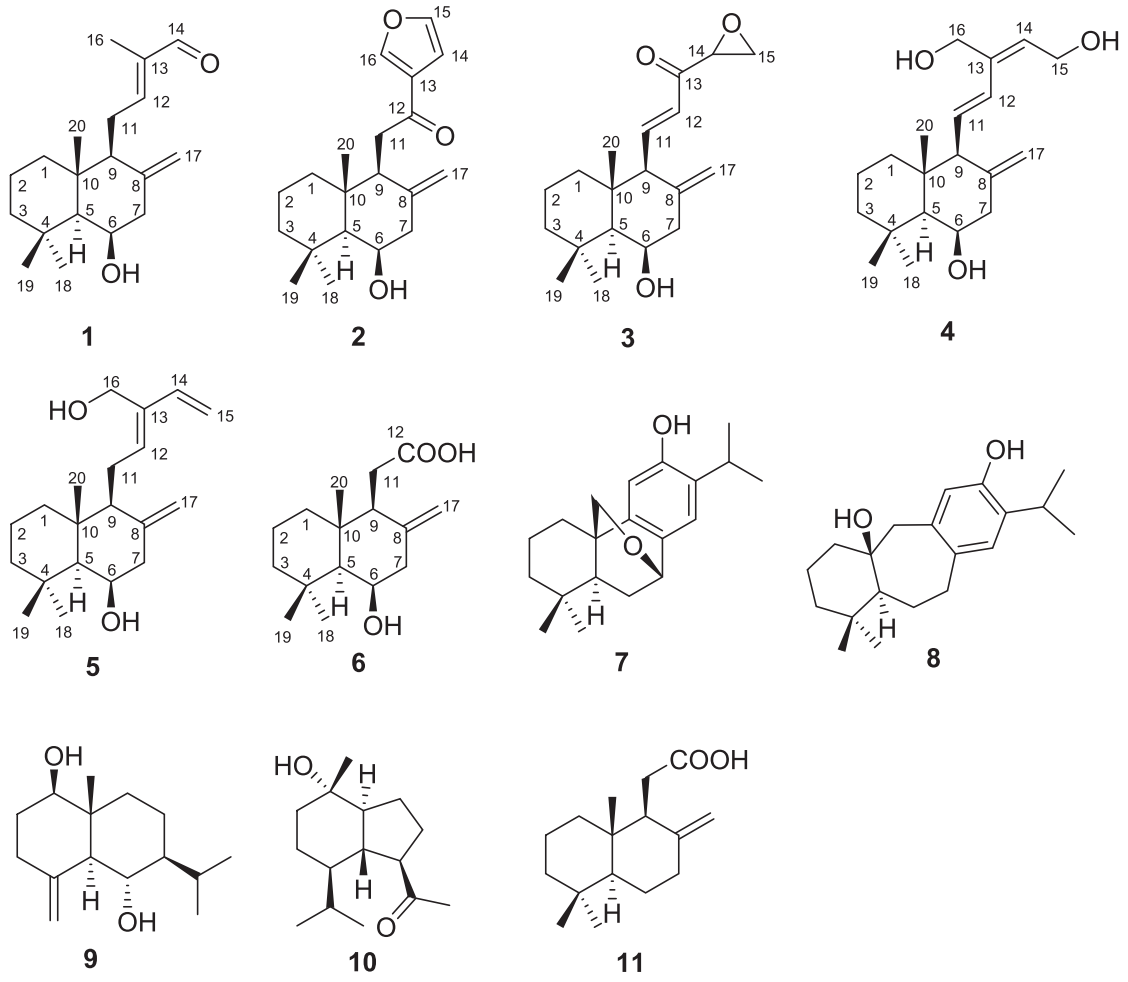

Fig. 1. Structures of compounds **1–11**.

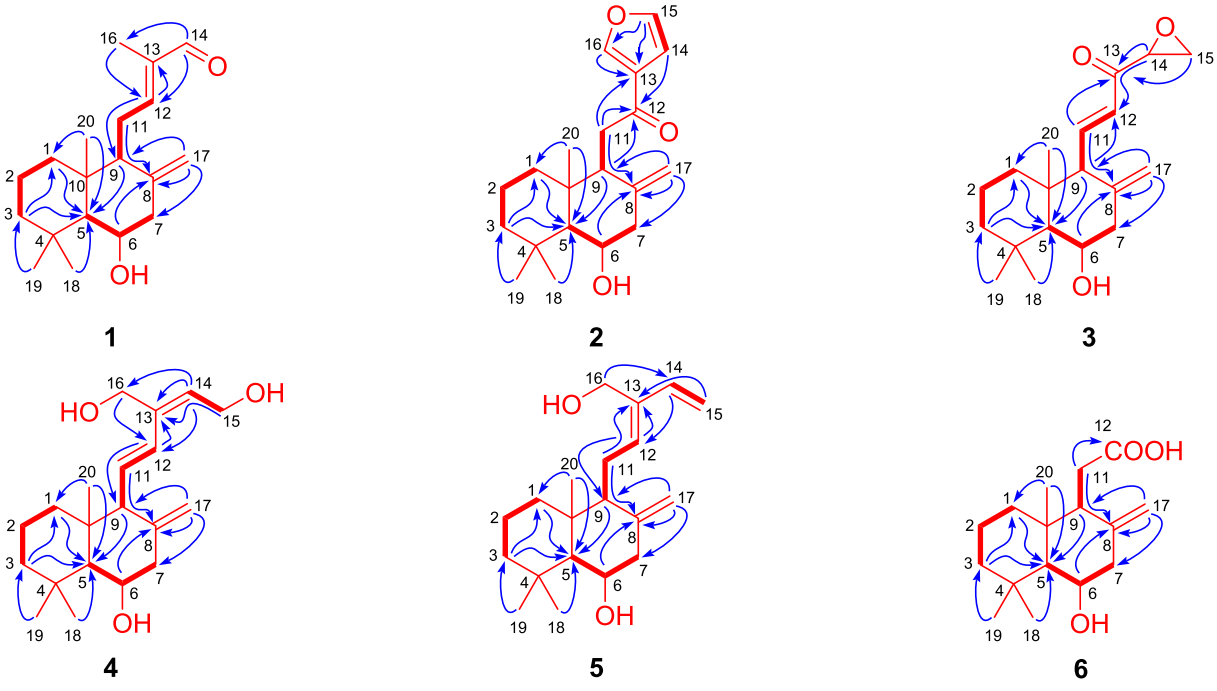

Fig. 2. ^{1}H-^{1}H COSY and key HMBC correlations of compounds **1–6**.

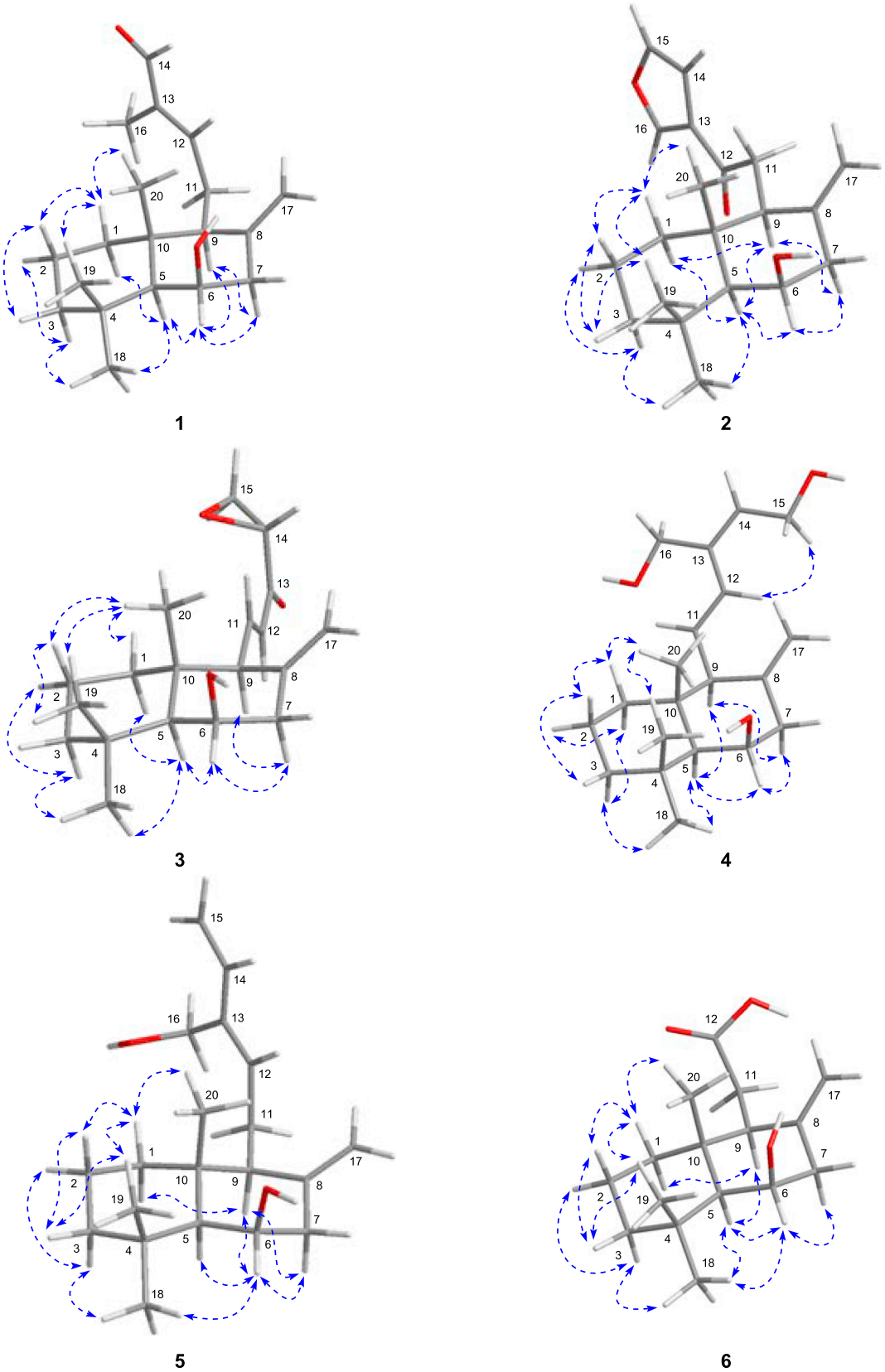

Fig. 3. Conformations and key NOESY correlations of compound **1–6**.

four olefinic protons (Table 2). The ^{13}C NMR spectrum showed 19 carbon resonances (Table 1) comprising three methyls, six methylenes [one olefinic methylene (δ_C 112.4) and one oxymethylene (δ_C 46.2)], six methines [two oxymethines (δ_C 68.7 and 52.9) and two olefinic methines (δ_C 126.1 and 148.4)], and four quaternary carbons [one ketone carbonyl (δ_C 195.0) and one olefinic carbon (δ_C 144.4)] with the aid of DEPT and HMQC spectra (Table 1). According to the typical aliphatic methyl singlets [δ_H 1.02 (H_3-18), 1.23 (H_3-19), and 1.21 (H_3-

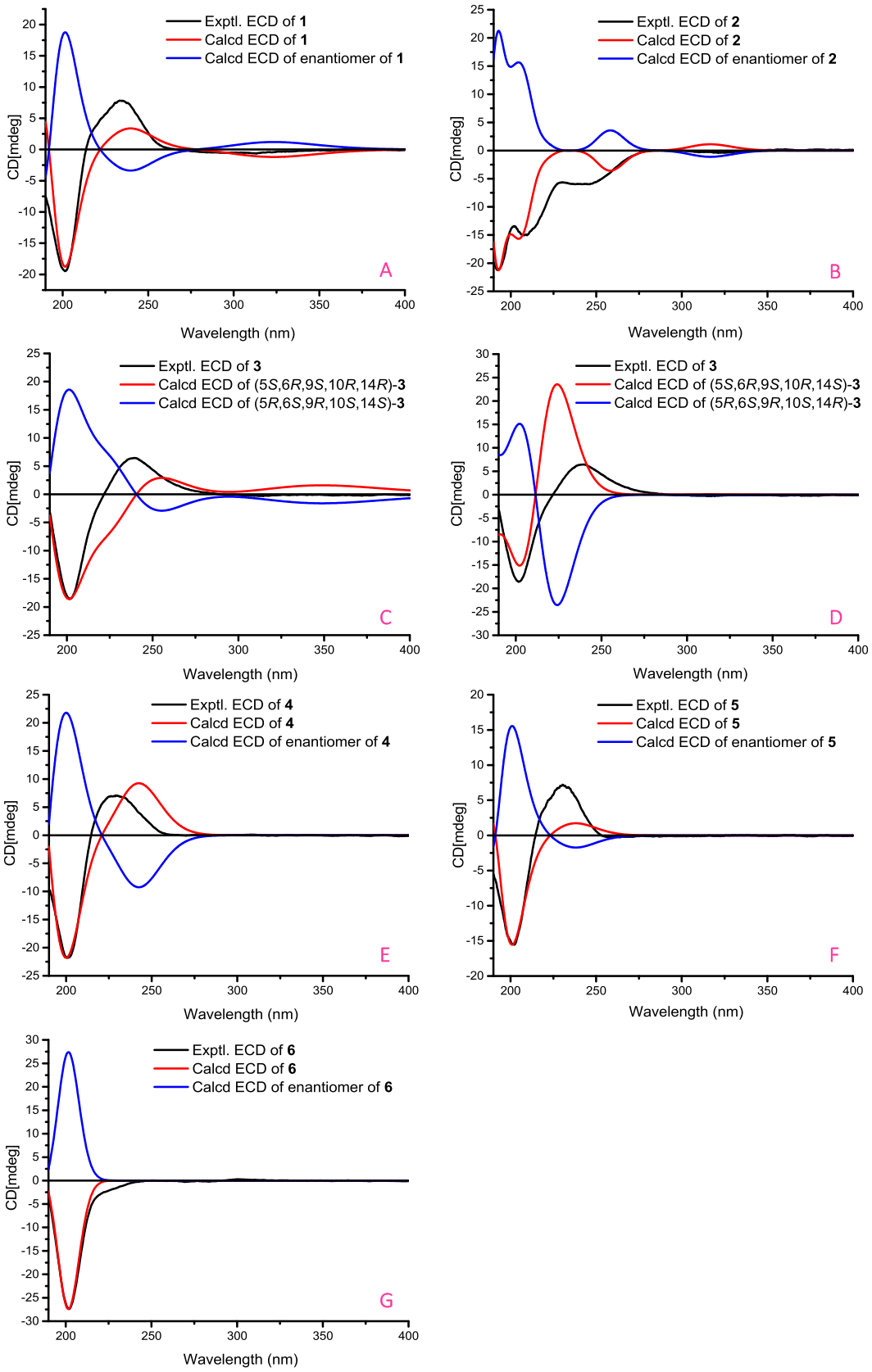

Fig. 4. Calculated and experimental ECD spectra of compounds **1** (A), **2** (B), **3** (C and D), **4** (E), **5** (F), and **6** (G) in acetonitrile.

20)] and the olefinic protons [4.69 and 4.96 (each 1H, s, H_2-17)] of the terminal double bond, the same 6/6 fused bicyclic fragment composed of C-1–C-10 and C-17–C-20 in compound **3** as those of **1** and **2** was extrapolated by comparison of chemical shifts of C-1–C-10 and C-17–C-20 in these compounds. This fragment was confirmed by the following HMBC and ^{1}H-^{1}H COSY experiments. In addition to the above fragment,

Table 3
IC_{50} values of compounds **1–11** inhibiting NO production in BV-2 cells.

Compound	IC_{50} (μM)[a]	Compound	IC_{50} (μM)
1	> 30[b]	**7**	> 10[b]
2	> 30[b]	**8**	> 10[b]
3	36.3 ± 7.1	**9**	> 100[b]
4	76.6 ± 1.2	**10**	> 100[b]
5	23.0 ± 1.0	**11**	45.0 ± 5.6
6	87.6 ± 11.5	SMT[a]	2.3 ± 0.1

[a] SMT (2-methyl-2-thiopseudourea, sulfate) was used as a positive control. Data are presented based on three experiments.

[b] The number with the superscript indicates the maximum concentration nontoxic to BV-2 cells, and the inhibitory rate on NO production is below 50% at this concentration.

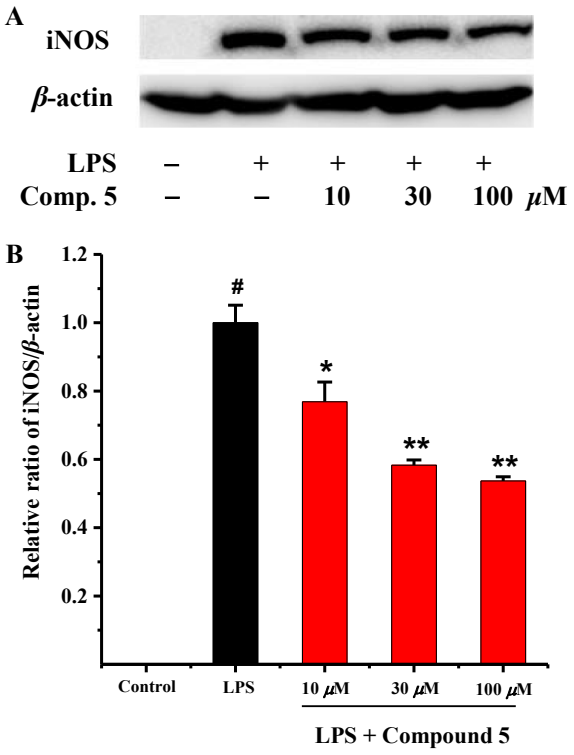

Fig. 5. Effects of compound **5** on iNOS protein expression in LPS-stimulated BV-2 cells. (A) Western blot images of iNOS in compound **5** (10, 30, 100 μM)-treated cells. The iNOS band intensities were quantified using NIH Image-J software (Bethesda, MD, USA). β-Actin was used as a loading control. (B) iNOS levels in culture media. #$p < 0.001$, significantly different from LPS-untreated sample, *$p < 0.05$, **$p < 0.01$, ***$p < 0.001$, significantly different from LPS-treated sample.

the remaining five carbon signals at δ_C 195.0, 148.4, 126.1, 52.9, and 46.2 were inferred to constitute a side chain by the ^{1}H-^{1}H COSY and HMBC correlations as shown in Fig. 2, where the signals at δ_C 148.4 (C-11), 126.1 (C-12), 195.0 (C-13), 52.9 (C-14), and 46.2 (C-15) were attributed. The above spectroscopic data analysis permitted seemingly the establishment of planar structure of **3**. However, this planar structure was not consistent with the molecular formula from the HRESIMS data, suggesting one more ring in this compound according to the total indices of hydrogen deficiency. According to the upfield chemical shifts of C-14 (δ_C 52.9) and C-15 (δ_C 46.2) and the corresponding proton signals [δ_H 3.58 (H-14), and 3.06 and 2.89 (each 1H, H_2-15)], a 14,15-epoxy moiety was proposed [38], as supported by the HEESIMS data. The NOESY data analysis disclosed that 6/6 fused bicyclic fragment presented the same conformation as those of compounds **1** and **2** and the C-6 hydroxy group was in a β-position. Due to lack of sufficient NOESY interactions between H-14 and other protons, the configuration of C-14 could not be able to determine. Then, the C-14 was hypothesized to be *rel-R* or *rel-S*, and the calculated ECD spectra of (5*S*,6*R*,9*S*,10*R*,14*R*)-**3** and (5*S*,6*R*,9*S*,10*R*,14*S*)-**3** were obtained respectively (Fig. 4). Both of the calculated ECD spectra matched the experimental data (Fig. 4), which means that the configuration of C-14 could still not be determined using TDDFT calculations. On the basis of the above analysis, the configuration of compound **3** was assigned as 5*S*, 6*R*, 9*S*, 10*R*, and 14ξ, and compound **3** was named euonymupene C.

Compound **4** possessed a molecular formula as $C_{20}H_{32}O_3$ based on its NMR data (Tables 1 and 2) and the HRESIMS ion at *m/z* 321.2433 $[M+H]^+$ (calcd for $C_{20}H_{33}O_3$, 321.2430). The ^{1}H NMR spectrum showed three aliphatic methyl singlets (δ_H 1.02, 1.14, and 1.23) and two olefinic protons (δ_H 4.74 and 4.93) attributable to a terminal double bond, which were similar to those of compounds **1–3**. The ^{13}C NMR spectra exhibited 20 carbon signals including three methyls, seven methylenes [two oxymethylenes (δ_C 58.6 and 64.7) and one olefinic methylene (δ_C 111.8)], six methines [one oxymethine (δ_C 69.0) and three olefinic methines (δ_C 126.3, 127.0, and 130.8)], and four quaternary carbons including two olefinic carbons (δ_C 137.9 and 145.9), based on the DEPT and HMQC spectra. These spectroscopic features indicated compound **4** to be also a labdane-type diterpenoid. Comparison of its NMR data with those of compounds **1–3**, the same 6/6 fused bicyclic fragment (C-1–C-10 and C-17–C-20) was proposed, which was confirmed by the following HMBC and ^{1}H-^{1}H COSY experiments. In addition to this moiety, the residual six signals including two oxymethylene and four olefinic carbons (δ_C 137.9, 130.8, 127.0, 126.3, 64.7, and 58.6) were found to form a side chain (C-11–C-16) as illustrated in Fig. 2 by interpretation of the HMBC and ^{1}H-^{1}H COSY data. This side chain was corroborated to be linked to C-9 indicated by the ^{1}H-^{1}H COSY correlations of H-9/H_2-11 and the corresponding HMBC correlations shown in Fig. 2. Further NMR spectroscopic data analysis allowed the proton and carbon signals to be assigned and a planar structure of labdane-type diterpenoid was established. The relative configuration of the 6/6 fused bicyclic moiety was the same as those of compounds **1–3** by analysis of its NOESY spectrum. The double bonds Δ^{11} and Δ^{13} were assigned as both *E*-configurations based on the coupling constants ($J_{11,12}$ = 15.3 Hz) and the NOESY correlations of H_2-16/H-11 and H-12/H_2-15. The absolute configuration was assigned as 5*S*, 6*R*, 9*S*, and 10*R*, by comparison of calculated and experimemtal ECD spectra, of which the former was obtained using TDDFT calculations. Hence, the structure of **4** was characterized and named euonymupene D.

The molecular formula of compound **5** was determined as $C_{20}H_{32}O_2$ based on the HRESIMS ion at *m/z* 305.2478 $[M+H]^+$ (calcd for $C_{20}H_{33}O_2$, 305.2481). The ^{1}H NMR spectra of **5** exhibited similar characteristic signals attributable to three aliphatic methyl singlets (δ_H 1.01, 1.04, and 1.21) and six olefinic protons [δ_H 6.26 (H-12), 5.61 (H-14), 5.29 and 5.02 (H_2-15), and 4.77 and 5.02 (H_2-17)]. The ^{13}C NMR spectrum showed 20 carbon resonances (Table 1). Its ^{1}H and ^{13}C NMR were similar to those of compound **4**, suggesting compound **5** should be a labdane-type diterpenoid structurally related to compound **4**. By comparing of its ^{13}C NMR data with those of compound **4**, the same 6/6 fused bicyclic moiety composed of C-1–C-10 and C-17–C-20 as present in compound **4** was inferred, which was substantiated by 2D NMR experiments. Apart from these 14 carbons for this moiety, the remaining six carbons were extrapolated to constitute a six-carbon side chain similar to that of compound **4**. By interpretation of HMBC and ^{1}H-^{1}H COSY data, the six-carbon side chain was confirmed and the olefinic and oxygenated carbons [δ_C 138.7(C-12), 136.8(C-13), 136.7(C-14), 111.5 (C-15), and 69.2(C-16)], as well as the other proton and carbon signals were attributed. A NOESY experiment revealed the conformation of two trans-fused six membered rings A and B, where H-5 and H-9 were α-axially oriented, and Me-19, Me-20, and the C-6 hydroxy group were β-axially oriented. After defining the relative configuration, the absolute configuration of **5** was deduced to be 5*S*, 6*R*, 9*S*, and 10*R*, by

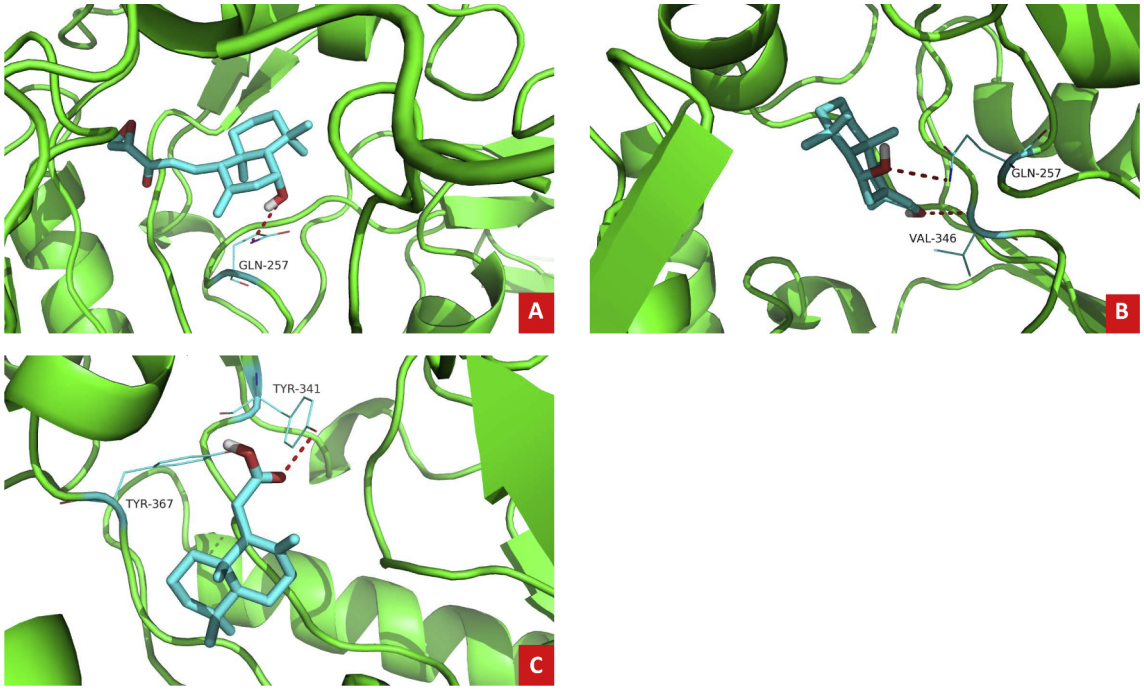

Fig. 6. Molecular docking simulations obtained at lowest energy conformation, highlighting potential hydrogen contacts of compounds **3** (A), **5** (B), and **11** (C), respectively. (Colored by atom: carbon is cyan; nitrogen is blue; oxygen is red; hydrogen is gray; sulfur is orange). For clarity, only interacting residues are labeled. Hydrogen bonding interactions are shown by dashes. These figures were created by PyMOL.

comparison of experimental ECD data with those calculated by TDDFT ECD calculations (Fig. 4). Compound **5** was therefore elucidated and given a trivial name euonymupene E.

The ^{1}H NMR spectra of **6** exhibited similar characteristic signals attributable to three aliphatic methyl singlets (δ_H 1.01, 1.01, and 1.20). The ^{13}C NMR spectrum showed 16 carbon resonances (Table 1). Analysis of 1D and 2D NMR spectra of compound **6** disclosed the 6/6 fused bicyclic fragment consisting of C-1–C-10 and C-17–C-20 (Fig. 2). There were two carbon signals left including one methylene (δ_C 30.7) and a carboxyl group (δ_C 179.5), which were attributed to C-11 and C-12, by analysis of the 2D NMR data. The NOESY experiment revealed that the 6/6 fused bicyclic fragment in **6** had the same conformation as that of compound **1**. After defining the relative configuration, the absolute configuration of compound **6** was established to be 5*S*, 6*R*, 9*S*, and 10*R*, by comparison of the experimental and calculated ECD data (Fig. 4). On the basis of the above evidence, the structure of **6** was elucidated as shown, and the compound, a labdane-type tetranorditerpenoid, was named euonymupene F.

By analysis of the NMR spectroscopic data and comparison with the literature, the remaining known compounds were elucidated as formosanoxide (**7**) [43], pisiferanol (**8**) [44], eudesm-4(15)-*ene*-1*β*,6*α*-diol (**9**) [45], oplopanone (**10**) [46], and 13, 14, 15, 16-tetranorlabda-8(17)-*en*-12-carboxylic acid (**11**) [47].

3.2. NO inhibitory activity

The discovery of bioactive substances plays an important role in the research and development of new drugs. NO is a signaling molecule and has been well known to regulate various physiological functions in many tissues of the human body [48]. To obtain NO inhibitory substances as potential lead compounds for inflammation, compounds **1–11** isolated from the twigs of *E. verrucosus* var. *pauciflorus* were assayed for their inhibitory activities on LPS-induced NO production in murine microglial BV-2 cells by the Griess reaction as described previously [49–51]. 2-Methyl-2-thiopseudourea, sulfate (SMT) was used as a positive control (IC_{50} value of 2.3 μM). All of these compounds exhibited inhibitory effects on LPS-induced NO production and the IC_{50} values were collated in Table 3. According to their IC_{50} values (Table 3), compounds **3**, **5**, and **11** exhibited moderate inhibition against LPS-induced NO production in BV-2 cells with IC_{50} values < 50 μM (Table 3). The (3-(4,5-dimethylthiazol-2-yl)-2,5-diphenyltetrazolium bromide (MTT) assay indicated that all of the compounds had no significant cytotoxicity to the BV-2 cells at their effective concentration for the inhibition of NO production (data not shown).

3.3. Evaluation of iNOS protein expression

NO was synthesized by three types of nitric oxide synthase (NOS): endothelial NOS (eNOS), neural NOS (nNOS), and inducible NOS (iNOS). It is well known that excessive NO production in inflammatory process is regulated by iNOS [52]. To further examine the mechanism of NO inhibitory effect of compound **5**, the most potent compound, western blotting analysis was used to evaluate the iNOS protein expression. As shown in Fig. 5, BV-2 cells treated by LPS (0.2 μg/mL), the expression of iNOS increased remarkably. While the cells were pretreated with the compound **5**, the protein expression were significantly decreased in a dose-dependent manner. The results exhibited that compound **5** inhibited the NO production by down-regulating the expression of iNOS protein.

3.4. Molecular docking studies

To understand the interactions between bioactive compounds and iNOS, molecular docking studies were applied to evaluate the binding abilities and sites of these bioactive diterpenoids with iNOS protein [38,39]. Compared with the other compounds, compounds **3**, **5**, and **11** showed more active NO inhibitory affects, which were selected for molecular docking investigations. As shown in Fig. 6, the three compounds exhibited strong affinities with iNOS. The binding free energies and sites were collated in Table 4.

Table 4
Logarithms of free binding energies (FBE, kcal/mol) of NO inhibitors to the active cavities of iNOS (PDB code: 3E6T) and targeting residues of the binding site located on the mobile flap.

Compound	−Log (FBE)	Targeting residues
3	−8.4	GLN-257
5	−8.0	VAL-346 GLN-257
11	−7.1	TYR-341 TYR-367

4. Conclusion

The results herein provide phytochemical and biological data concerning the terpenoids isolated from the twigs of *Euonymus verrucosus* var. *pauciflorus*. Six new diterpenoids (**1–6**) and five known compounds (**7–11**) have been isolated. Their structures were elucidated on the basis of extensive 1D and 2D NMR spectroscopic data analysis, and TDDFT ECD calculations. All of the isolates were evaluated biologically for the NO inhibition in LPS-induced murine microglial BV-2 cells, and compounds **3**, **5**, and **11** exerted more inhibition against NO production compared to the other compounds. Western blotting analysis indicated compound **5**, the most potent compound, exhibited the anti-inflammatory effect by down-regulating iNOS protein. The further studies of molecular docking revealed that compounds **3**, **5**, and **11** have strong affinities with the iNOS protein by targeting residues of the active cavities of iNOS. The discovery of these bioactive terpenoids suggested that the twigs of *E. verrucosus* var. *pauciflorus* have the potential medicinal value for treatment of inflammation.

Acknowledgments

This research was supported by the National Key Research and Development Program of China (No. 2018YFA0507204), the Natural Science Foundation of Tianjin, China (No. 16JCYBJC27700), National Natural Science Foundation of China (Nos. U1703107, 21642016, and 21372125), Hundred Young Academic Leaders Program of Nankai University, State Key Laboratory for Chemistry and Molecular Engineering of Medicinal Resources (Guangxi Normal University, No. CMEMR2018-B02), and the Fundamental Research Funds for the Central Universities.

Appendix A. Supplementary material

Supplementary data to this article can be found online at https://doi.org/10.1016/j.bioorg.2019.03.022.

References

[1] S.R. Lee, S. Lee, E. Moon, H.J. Park, H.B. Park, K.H. Kim, Bioorg. Chem. 70 (2017) 94–99.
[2] M.C. Seguin, F.W. Klotz, I. Schneider, J.P. Weir, M. Goodbary, M. Slayter, J.J. Raney, J.U. Aniagolu, S.J. Green, J. Exp. Med. 180 (1994) 353–358.
[3] P. Pacher, J.S. Beckman, L. Liaudet, Physiol. Rev. 87 (2007) 315–424.
[4] Y. Tang, Z.Z. Zhao, J.N. Yao, T. Feng, Z.H. Li, H.P. Chen, J.K. Liu, J. Nat. Prod. 81 (2018) 2163–2168.
[5] C.Q. Li, B. Pang, T. Kiziltepe, L.J. Trudel, B.P. Engelward, P.C. Dedon, G.N. Wogan, Chem. Res. Toxicol. 19 (2006) 399–406.
[6] N.B. Ghate, D. Chaudhuri, S. Panja, S.S. Singh, G. Gupta, C.Y. Lee, N. Mandal, J. Nat. Prod. 81 (2018) 1956–1961.
[7] Editorial Committee of the Flora of China, Chinese Academy of Sciences, Flora of China 45, 1999, 54.
[8] Z.F. Fang, Z.L. Li, Y. Wang, W. Li, H.M. Hua, Chin. Tradit. Herbal Drugs 38 (2011) 810–812.
[9] M.P. Simmons, V. Savolainen, C.C. Clevinger, R.H. Archer, J.I. Davis, Mol. Phylogenet. Evol. 19 (2001) 353–366.
[10] G.H. Tu, X.W. Shi, Y. Zhao, C.D. Zheng, J.M. Gao, Chem. Nat. Compd. 47 (2011) 656–657.
[11] J.X. Zhu, J.J. Qin, R.J. Chang, Q. Zeng, X.R. Cheng, F. Zhang, H.Z. Jin, W.D. Zhang, Chem. Biodivers. 9 (2012) 1055–1076.
[12] J. Zhu, M. Wang, W. Wu, Z. Ji, Z. Hu, Phytochemistry 61 (2002) 699–704.
[13] Y.H. Kuo, H.C. Huang, W.F. Chiou, L.S. Shi, T.S. Wu, Y.C. Wu, J. Nat. Prod. 66 (2003) 554–557.
[14] H. Wang, X. Tian, Y. Pan, Helv. Chim. Acta. 86 (2003) 3320–3325.
[15] Z.L. Liu, Z.J. Jia, X. Tian, H. Wang, Planta Med. 70 (2004) 353–358.
[16] H.C. Ko, Y.H. Kuo, B.L. Wei, W.F. Chiou, Planta Med. 71 (2005) 514–519.
[17] H. Wang, X. Tian, Chem. Pharm. Bull. 37 (2006) 219–221.
[18] J.M. Gao, W.J. Wu, J.W. Zhang, Y. Konishi, Nat. Prod. Rep. 24 (2007) 1153–1189.
[19] Y.D. Yang, G.Z. Yang, M.C. Liao, Z.N. Mei, Helv. Chim. Acta. 94 (2011) 1139–1145.
[20] F. Li, C.J. Li, J.Z. Yang, D.M. Zhang, J. Asian Nat. Prod. Res. 14 (2012) 755–758.
[21] J.X. Zhu, J. Ren, J.J. Qin, X.R. Cheng, Q. Zeng, F. Zhang, S.K. Yan, H.Z. Jin, W.D. Zhang, Arch. Pharm. Res. 35 (2012) 1739–1747.
[22] Y. Inaba, T. Hasuda, Y. Hitotsuyanagi, Y. Aoyagi, N. Fujikawa, A. Onozaki, A. Watanabe, T. Kinoshita, K. Takeya, J. Nat. Prod. 76 (2013) 1085–1090.
[23] D.C. Kim, T.H. Quang, N.T. Ngan, C.S. Yoon, J.H. Sohn, J.H. Yim, Y. Feng, Y. Che, Y.C. Kim, H. Oh, J. Nat. Prod. 78 (2013) 2948–2955.
[24] M.A. Tantry, A. Idris, I.A. Khan, Fitoterapia 89 (2013) 58–67.
[25] Z.H. Yan, Z.Z. Han, X.Q. Hu, Q.X. Liu, W.D. Zhang, R.H. Liu, H.L. Li, Helv. Chim. Acta. 96 (2013) 85–92.
[26] J. Zhou, C.J. Li, J.Z. Yang, J. Ma, Y. Li, X.Q. Bao, X.G. Chen, D. Zhang, D.M. Zhang, J. Nat. Prod. 77 (2014) 276–284.
[27] J. Alarcon, C.L. Cespedes, E. Munoz, C. Balbontin, F. Valdes, M. Gutierrez, L. Astudillo, D.S. Seigler, J. Agric. Food Chem. 63 (2015) 10250–10256.
[28] L.H. Yan, X.Q. Liu, H. Zhu, Q.R. Xu, W.M. Wang, S.M. Zhang, Q.W. Zhang, S.S. Zhang, Z.M. Wang, J. Asian Nat. Prod. Res. 17 (2015) 952–958.
[29] S. Lee, E. Moon, S.U. Choi, K.H. Kim, Chem. Biodivers. 13 (2016) 1391–1396.
[30] F. Li, J. Ma, C.J. Li, J.Z. Yang, D. Zhang, X.G. Chen, D.M. Zhang, Phytochemistry 135 (2017) 144–150.
[31] J. Zhou, X. Wei, F. Chen, C. Li, J. Yang, J. Ma, X. Bao, D. Zhang, D. Zhang, Fitoterapia 118 (2017) 21–26.
[32] MOE, Chemical Computing Group Inc., 2013, http://www.chemcomp.com.
[33] M.J. Frisch, G.W. Trucks, H.B. Schlegel, G.E. Scuseria, M.A. Robb, J.R. Cheeseman, G. Scalmani, V. Barone, B. Mennucci, G.A. Petersson, H. Nakatsuji, M. Caricato, X. Li, H.P. Hratchian, A.F. Izmaylov, J. Bloino, G. Zheng, J.L. Sonnenberg, M. Hada, M. Ehara, K. Toyota, R. Fukuda, J. Hasegawa, M. Ishida, T. Nakajima, Y. Honda, O. Kitao, H. Nakai, T. Vreven, J.A. Montgomery Jr., J.E. Peralta, F. Ogliaro, M. Bearpark, J.J. Heyd, E. Brothers, K.N. Kudin, V.N. Staroverov, R. Kobayashi, J. Normand, K. Raghavachari, A. Rendell, J.C. Burant, S.S. Iyengar, J. Tomasi, M. Cossi, N. Rega, J.M. Millam, M. Klene, J.E. Knox, J.B. Cross, V. Bakken, C. Adamo, J. Jaramillo, R. Gomperts, R.E. Stratmann, O. Yazyev, A.J. Austin, R. Cammi, C. Pomelli, J.W. Ochterski, R.L. Martin, K. Morokuma, V.G. Zakrzewski, G.A. Voth, P. Salvador, J.J. Dannenberg, S. Dapprich, A.D. Daniels, O. Farkas, J.B. Foresman, J.V. Ortiz, J. Cioslowski, D.J. Fox, Gaussian 09, Revision B.01, Gaussian Inc., Wallingford, CT, 2010.
[34] T. Bruhn, A. Schaumlöffel, Y. Hemberger, G. Bringmann, SpecDis, Version 1.62, University of Wuerzburg, Germany, 2014.
[35] K.H. Kim, S.K. Ha, S.U. Choi, S.Y. Kim, K.R. Lee, Planta Med. 79 (2013) 361–364.
[36] H. Wang, Y. Liu, J. Zhang, J. Xu, C.A. Cui, Y. Guo, D.Q. Jin, Neurosci. Lett. 612 (2017) 149–154.
[37] E.D. Garcin, A.S. Arvai, R.J. Rosenfeld, M.D. Kroeger, B.R. Crane, G. Andersson, G. Andrews, P.J. Hamley, P.R. Mallinder, D.J. Nicholls, S.A. St-Gallay, A.C. Tinker, N.P. Gensmantel, A. Mete, D.R. Cheshire, S. Connolly, D.J. Stuehr, A. Aberg, A.V. Wallace, J.A. Tainer, E.D. Getzoff, Nat. Chem. Biol. 4 (2008) 700–707.
[38] M. Chayah, M.D. Carrión, M.A. Gallo, R. Jiménez, J. Duarte, M.E. Camacho, ChemMedChem 10 (2015) 874–882.
[39] S. Li, X. Sun, Y. Li, F. Liu, J. Ma, L. Tong, G. Su, J. Xu, Y. Ohizumi, D. Lee, Y. Guo, Bioorg. Med. Chem. Lett. 27 (2017) 670–674.
[40] L.K. Sy, G.D. Brown, J. Nat. Prod. 60 (1997) 904–908.
[41] X.C. Li, D. Ferreira, Y. Ding, Curr. Org. Chem. 14 (2010) 1678–1697.
[42] J. Xu, J. Kang, X. Sun, X. Cao, K. Rena, D. Lee, Q. Ren, S. Li, Y. Ohizumi, Y. Guo, J. Nat. Prod. 79 (2016) 170–179.
[43] K.C. Hsu, J.M. Fang, Y.S. Cheng, J. Nat. Prod. 58 (1995) 1592–1595.
[44] S. Hasegawa, T. Kojima, Y. Hirose, Phytochemistry 24 (1985) 1545–1551.
[45] H.J. Zhang, G.T. Tan, B.D. Santarsiero, A.D. Mesecar, N.V. Hung, N.M. Cuong, D.D. Soejarto, J.M. Pezzuto, H.H.S. Fong, J. Nat. Prod. 66 (2003) 609–615.
[46] K.Y. Jung, D.S. Kim, S.R. Oh, I.S. Lee, J.J. Lee, H.K. Lee, D.H. Shin, E.H. Kim, C.J. Cheong, Arch. Pharm. Res. 20 (1997) 363–367.
[47] Q. Zhao, X.J. Hao, C. Zou, R.P. Zhang, J.L. Hu, Nat. Prod. Res. Dev. 21 (2009) 10–12.
[48] B. Liu, H.M. Gao, J.Y. Wang, G.H. Jeohn, C.L. Cooper, J.S. Hong, Ann. N. Y. Acad. Sci. 962 (2002) 318–331.
[49] F. Liu, X. Yang, Y. Liang, B. Dong, G. Su, M. Tuerhong, D.Q. Jin, J. Xu, Y. Guo, Phytochemistry 147 (2018) 57–67.
[50] J. Xu, F. Ji, J. Kang, H. Wang, S. Li, D.Q. Jin, Q. Zhang, H. Sun, Y. Guo, J. Agric. Food Chem. 63 (2015) 5805–5812.
[51] W.S. Suh, K.J. Park, D.H. Kim, L. Subedi, S.Y. Kim, S.U. Choi, K.R. Lee, Bioorg. Chem. 72 (2017) 156–160.
[52] S.R. Lee, S. Lee, E. Moon, H.J. Park, H.B. Park, K.H. Kim, Bioorg. Chem. 70 (2016) 94–99.